Characterizing Genetically Altered Mouse Models—Pathology

This article has been reproduced from *Toxicologic Pathology*, Volume 26, No. 4, pp. 501-511, 1998, with the permission of The Society of Toxicologic Pathology.

Spontaneous and Chemically Induced Proliferative Lesions in Tg.AC Transgenic and *p53*-Heterozygous Mice*

JOEL F. MAHLER,[1] NORRIS D. FLAGLER,[1] DAVID E. MALARKEY,[2] PETER C. MANN,[3] JOSEPH K. HASEMAN,[1] AND WILLIAM EASTIN[1]

[1]*National Institute of Environmental Health Sciences, Research Triangle Park, North Carolina 27709*
[2]*North Carolina State University College of Veterinary Medicine, Raleigh, North Carolina 27606*
[3]*Experimental Pathology Laboratories, Inc., Research Triangle Park, North Carolina 27709*

ABSTRACT

Recently, the use of selected genetically altered mouse models in the detection of carcinogens after short-term chemical exposures has been evaluated. Studies of several chemicals conducted by the National Toxicology Program in Tg.AC transgenic and heterozygous *p53*-deficient mice have been completed recently and represent a major contribution to this effort, as well as the largest accumulation to date of toxicologic pathology data in these 2 lines of mice. The purpose of this report is to describe the proliferative target organ effects observed in this set of studies, as well as to present the tumor profile in the control groups of this data set. These findings provide a comprehensive toxicologic assessment of these 2 genetically altered mouse strains, which are of emerging importance in toxicologic pathology.

Keywords. Mice; genetically altered; hazard identification; neoplasms; carcinogenicity

INTRODUCTION

As part of the global initiative to examine the utility of genetically altered mice in the detection of carcinogens in short-term studies, the National Institute of Environmental Health Sciences (NIEHS) and the National Toxicology Program (NTP) have conducted a series of studies to further characterize these models, with focus on the Tg.AC transgenic and heterozygous *p53*-deficient (+/−) lines. The rationale behind this initiative as well as the choice of these 2 lines is described in detail by Eastin et al in this issue (8). Descriptions of some of the spontaneously formed lesions found in Tg.AC and $p53^{+/-}$ mice have previously been published (3, 6), as have descriptions of the sensitivity of the Tg.AC line to detect skin carcinogens by a skin papilloma phenotype (20). As an extension of these studies, Tennant et al (21) proposed a 2-model paradigm that utilized the Tg.AC and $p53^{+/-}$ systems as a means to identify chemicals with carcinogenic potential, and this paradigm formed the basis for the NTP effort as described by Eastin et al (8). The purpose of this report is to describe in more detail the spontaneous and chemically induced lesions observed in these 2 lines of mice using these NTP studies as the data set.

MATERIALS AND METHODS

The mice used in these studies were obtained from Taconic Farms (Germantown, NY) at 4–5 wk of age and were placed on test at approximately 7 wk of age. The Tg.AC line was derived from pronuclear injection of FVB/N strain zygotes with an activated v-Ha-*ras* containing construct. Homozygous Tg.AC males were mated to FVB/N females and the heterozygous Tg.AC progeny were used for these studies. Heterozygous *p53*-deficient mice have 1 disrupted *p53* allele as the result of gene targeting in embryonic stem cells. $p53^{+/-}$ mice used in the current studies were on a C57BL/6 genetic background. The chemical and dose selection rationale, experimental design, and in-life procedures of these studies are described in detail by Eastin et al (8). The individual studies in $p53^{+/-}$ and Tg.AC transgenic mice that comprise the current data set are summarized in Table I. These include retrospective studies of 11 chemicals with known human or rodent carcinogenic activity, 1 shaving control study in Tg.AC mice of both sexes, and prospective studies of 2 chemicals in female Tg.AC mice only.

Complete necropsies were conducted on all mice at terminal sacrifice following the 6-mo exposure period, as well as on all animals that died natural deaths and on those animals sacrificed for humane reasons. All tissues were preserved in 10% neutral-buffered formalin. Protocol-required tissues were processed through paraffin, cut in 5–6 μm sections, and stained with hematoxylin and eosin. Because the retrospective and prospective studies were conducted at different times, there was a slight variation in the protocol-required tissues for microscopic examination. For the retrospective studies, these

* Address correspondence to: Dr. Joel Mahler, NIEHS, Mail Drop B3-06, P.O. Box 12233, Research Triangle Park, North Carolina 27709.

0192-6233/98$3.00+$0.00

TABLE I.—NTP-sponsored chemical studies in Tg.AC transgenic and $p53^{+/-}$ mice.

	Tg.AC	*p53*
Retrospective		
Cyclosporin	Gavage	Gavage
2,4-Diaminotoluene	Topical	Feed
2,6-Diaminotoluene	Topical	Feed
Diethylstilbestrol	Topical	Subcutaneous injection
8-Hydroxyquinoline	Topical	Feed
Melphalan	Topical	Intraperitoneal injection
N-Methylolacrylamide	Gavage	—[a]
N-Methylolacrylamide	Topical	—
p-Anisidine	Topical	—[a]
Resorcinol	Topical	Gavage
Rotenone	Topical	Feed
2,3,7,8-Tetrachlorodibenzodioxin	Topical	Gavage
Negative control	Shaving	
Prospective		
Dicyclohexylcarbodiimide	Topical; females only	
Diisopropylcarbodiimide	Topical; females only	

[a] Study previously done and reported as negative by Spalding et al (20).

tissues were from liver, kidneys, spleen, stomach, lungs, thymus, lymph nodes (mandibular, mesenteric, and mediastinal), endocrine organs (adrenal, pituitary, and thyroid glands), ovary and uterus or testes and epididymides, gross lesions, skin site of application (SOA) (topical studies), and target sites of known carcinogens if not included in the above list. This tissue list allowed for the examination of known chemical-specific target sites identified in standard 2-yr bioassays and efficient screening for new targets unique to the $p53^{+/-}$ and Tg.AC strains by evaluation of a spectrum of tissues representing the majority of the target sites known for rodent carcinogenic activity (12). For the 2 prospective studies in this data set, a complete histopathologic examination was performed according to standard NTP protocol (4).

Peer review of the study pathologist's findings was first conducted by an independent reviewing pathologist. The reviewing pathologist reexamined all target organs for carcinogenic activity identified in the 2-yr bioassay (retrospective studies), determined the existence of any new target organs for neoplastic or nonneoplastic effects identified in the $p53^{+/-}$ and Tg.AC mouse models, and identified all neoplasms from all animals. A pathology working group was then conducted in order to review the pathology data from all studies, to microscopically confirm all neoplastic treatment effects and tumors in control animals, to resolve diagnostic differences between the study and reviewing pathologists, and to suggest appropriate terminology for unusual neoplasms.

TABLE II.—Summary of tumors in control Tg.AC transgenic and $p53^{+/-}$ mice.

Tumor	Incidence (%) Male	Female
Tg.AC mice[a]		
Odontogenic tumor	21 (13.0)	32 (17.3)
Forestomach papilloma	12 (7.4)	19 (10.3)
Skin papilloma	6 (3.7)	7 (3.8)
Skin carcinoma	0	1 (0.5)
Lung AB adenoma	7 (4.3)	3 (1.6)
Lung AB carcinoma	0	1 (0.5)
Salivary gland duct carcinoma	2 (1.2)	4 (2.2)
Erythroleukemia	1 (0.6)	4 (2.2)
Ovary teratoma	—	3 (1.6)
Malignant lymphoma	0	2 (1.1)
Endometrial adenoma	—	1 (0.5)
Uterine histiocytic sarcoma	—	1 (0.5)
Intestinal carcinoma	0	1 (0.5)
Subcutis mast cell tumor	0	1 (0.5)
$p53^{+/-}$ mice[b]		
Skin/subcutis sarcoma	2 (1.9)	4 (3.7)
Malignant lymphoma	2 (1.9)	2 (1.8)
Osteosarcoma	2 (1.9)	0
Granulocytic leukemia	1 (0.9)	0
Meningeal sarcoma	0	1 (0.9)
Lung adenoma	0	1 (0.9)
Urinary bladder sarcoma	1 (0.9)	0

[a] Tg.AC mice—male: n = 162; female: n = 185.
[b] $p53^{+/-}$ mice—male: n = 108; female: n = 109.

RESULTS

The spontaneous and treatment-related neoplastic effects observed in Tg.AC transgenic and $p53^{+/-}$ mice in NTP 26-wk studies are summarized in Tables II and III, respectively. Treatment-related tumor incidence data for the individual studies and a discussion of the concordance between these studies and the corresponding 2-yr bioassays can be found in the article by Eastin et al in this issue (8).

TABLE III.—Summary of treatment-related proliferative effects in Tg.AC transgenic and $p53^{+/-}$ mice.

Lesion	Study
Tg.AC transgenic mice	
Skin SOA—squamous cell papilloma/keratoacanthoma	Cyclosporin
	Dicyclohexylcarbodiimide
	Diethylstilbestrol
	Melphalan
	Resorcinol
	TCDD
Skin SOA—squamous cell carcinoma	Dicyclohexylcarbodiimide
	TCDD
	2,4-Diaminotoluene
Forestomach—squamous cell papilloma	Melphalan
	Cyclosporin
Lung—Adenoma/carcinoma	Melphalan
Systemic—malignant lymphoma	Cyclosporin
Systemic—myelodysplasia	Rotenone
$p53^{+/-}$ mice	
Soft tissues—sarcoma	Melphalan
Systemic—malignant lymphoma	Melphalan

Abbreviation: TCDD = 2,3,7,8-tetrachlorodibenzodioxin.

Tumors in Control Tg.AC and p53$^{+/-}$ Mice

The types of tumors found in control mice within this set of studies and their incidences are summarized in Table 2. In Tg.AC mice, odontogenic tumors were the most common spontaneous neoplasm, occurring in both sexes at an incidence of 13–17%. Odontogenic tumors were grossly evident as firm masses of the mandible or maxilla (Fig. 1). Consistent with a previous report in another population of Tg.AC mice (22), 3 distinct morphological types of odontogenic tumor were seen microscopically. One type appeared to arise from the periodontal ligament and was composed of mesenchymal cells embedded in a dense eosinophilic matrix (Fig. 2). Other tumors contained abortive tooth structures formed by enamel, dentine, and well-differentiated ameloblasts and odontoblasts, resembling true odontomas (Fig. 3). A third type of odontogenic tumor consisted of anastomosing cords of squamous cells surrounded by loose, undifferentiated stroma (Fig. 4). Some palisading of the basal cell nuclei in the epithelial cords of these tumors suggested ameloblastoma. Some tumors had areas with combinations of these characteristics (Fig. 5).

Tumors of the forestomach, skin, and lung were relatively common spontaneous neoplasms in control Tg.AC mice. Tumors at these sites were also treatment effects as described below, and morphologically the control neoplasms were identical to their treatment-related counterparts. After odontogenic tumors, the second most common tumor found in control Tg.AC mice was squamous papilloma of the forestomach. These tumors had a typical gross appearance of an exophytic growth visible on the opened mucosal surface. An incidence of 7–10% was observed in both sexes in this set of studies. However, approximately one-half of all forestomach papillomas in control Tg.AC mice unexplainedly occurred in a single study (2,6-diaminotoluene). No squamous carcinomas of the forestomach were found.

Squamous tumors of the skin and alveolar-bronchiolar (AB) tumors of the lung occurred with approximately equal frequency (2–4%) in male and female control Tg.AC mice. Squamous papillomas of the skin occurred at random sites. A single control female had a cutaneous squamous cell carcinoma and another control female had a lung AB carcinoma.

Two unusual neoplasms, squamous carcinoma of the salivary gland and erythroleukemia, occurred at a 1–2% incidence in male and female Tg.AC mice. Squamous cell carcinoma of the salivary gland was presumably of ductal origin and grossly appeared as a soft, fluctuant mass in the submandibular region. The tumor was typically cystic and contained thick mucoid material. The walls of the cyst were lined by well-differentiated, nonkeratinizing stratified squamous epithelium (Fig. 6). More peripherally there was usually an invasion into surrounding tissue by more anaplastic spindle cells. The larger tumors were several millimeters in diameter. Only with the smaller tumors could origin from within the salivary gland be detected. Both submandibular and sublingual glands appeared to be sites of origin.

Another unusual neoplasm seen in several control Tg.AC mice was erythroleukemia. Hepatomegaly due to severe sinusoidal and periportal cellular infiltration was a distinctive characteristic of affected animals (Fig. 7). Cytological features that distinguished this neoplastic infiltration were the presence of nucleated red blood cells mixed with undifferentiated blast cells that have slightly more basophilic cytoplasm than do lymphocytes. In addition to the liver, involvement of the spleen, bone marrow, and lymph node was common. Hypercellularity was noted in many vessels, in particular the capillaries of the lung parenchyma and the renal glomeruli. In a few animals, excessive numbers and/or size of erythropoietic foci were found in the liver and were interpeted to be incipient cases of erythroleukemia (Fig. 8).

→

FIGS. 1–8.—1) Low magnification of an odontogenic tumor arising from the periodontal area of the mandible. 2) Higher magnification of the tumor in Fig. 1, demonstrating mesenchymal cells embedded in a dense matrix. A nest of epithelial cells is in the top right of the field. 3) Odontogenic tumor resembling odontoma in a Tg.AC mouse, with hard matrix material forming multiple abortive tooth structures. 4) Odontogenic tumor resembling ameloblastoma in a Tg.AC mouse, with anastomosing squamous epithelial cords, cysts, and loose intervening stroma. 5) Odontogenic tumor in a Tg.AC mouse with components resembling both ameloblastoma and odontoma. 6) Ductal carcinoma arising within the submandibular salivary gland of a Tg.AC mouse with well-differentiated squamous epithelium on the right and more anaplastic, spindle epithelial cells in the middle, adjacent to gland lobules.7) Erythroleukemia in the liver of a Tg.AC mouse with sinusoidal dilatation and infiltration by basophilic undifferentiated blast cells and small red blood cell ponds with dark-staining metarubricytes. 8) Aberrant erythropoiesis in the liver of a Tg.AC mouse, interpreted to be incipient erythroleukemia.

→

FIGS. 9–16.—9) Tg.AC mouse with multiple skin papillomas at the site of chemical application. 10) Subgross photomicrograph of a typical exophytic, pedunculated squamous papilloma in a Tg.AC mouse. 11) Higher magnification of the papilloma in Fig. 10 showing well-differentiated squamous epithelium and intact basement membrane zone. 12) Keratoacanthoma at the skin site of chemical application in a Tg.AC mouse, with cup-shaped, endophytic growth. 13) Subgross photomicrograph of a squamous papilloma (from a Tg.AC mouse) converting to a squamous cell carcinoma. There is marked irregularity of the basal layer and multiple nests of epithelial cells in the stalk. 14) Higher magnification of the early carcinoma in Fig. 13 demonstrating invasive nests of moderately well-differentiated keratinocytes. 15) Subgross photomicrograph of a squamous papilloma (from a Tg.AC mouse) converting to a spindle cell carcinoma. There is surface ulceration and a dense population of tumor cells in the stalk. 16) Higher magnification of the tumor in Fig. 15. Note the abrupt transition between nests of proliferative squamous cells and the spindle cells of anaplastic carcinoma.

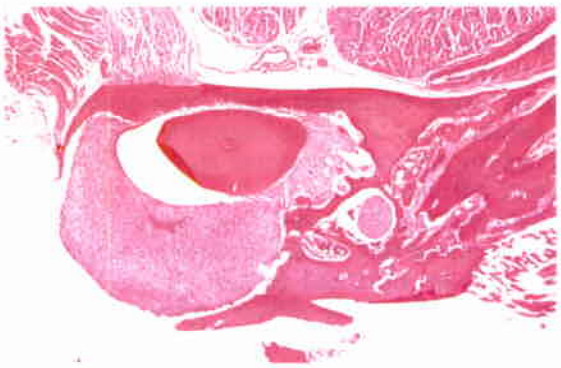

Figure 1

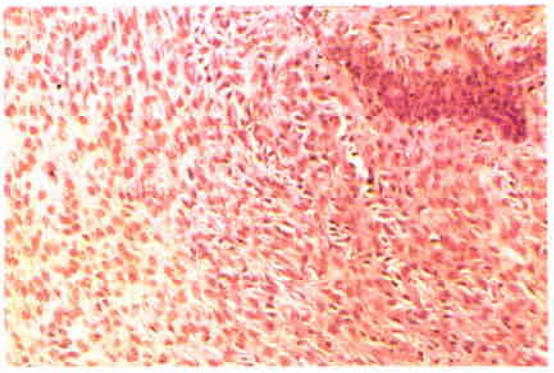

Figure 2

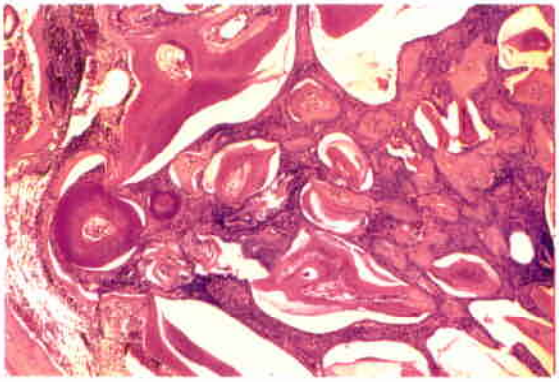

Figure 3

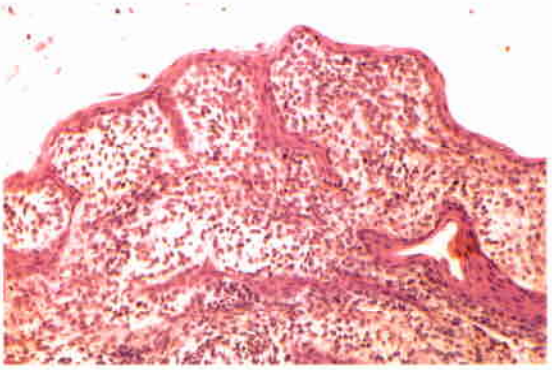

Figure 4

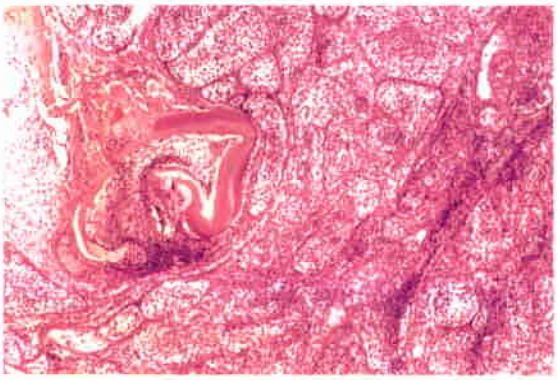

Figure 5

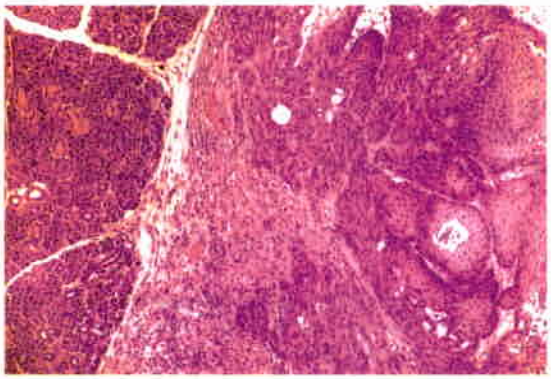

Figure 6

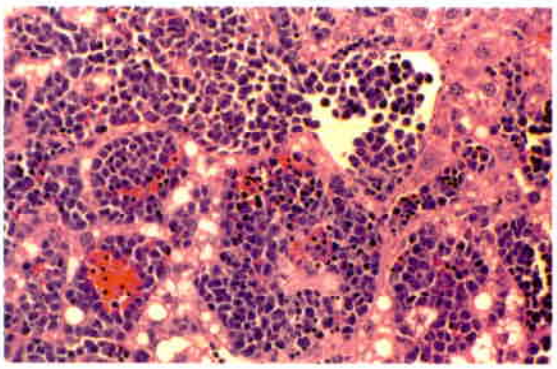

Figure 7

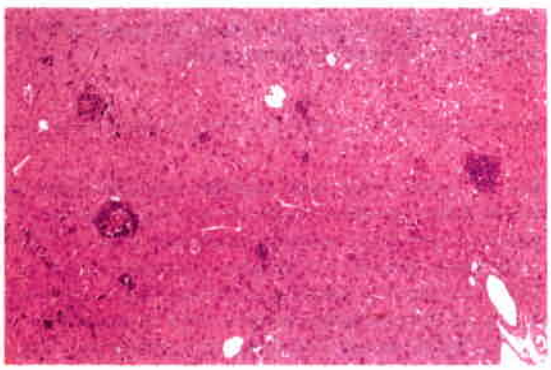

Figure 8

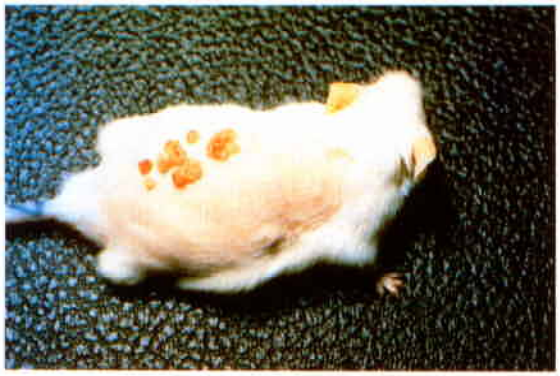

Figure 9

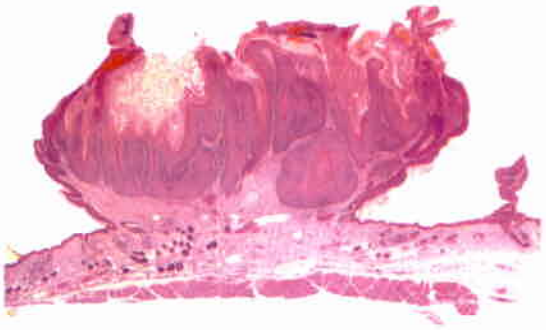

Figure 10

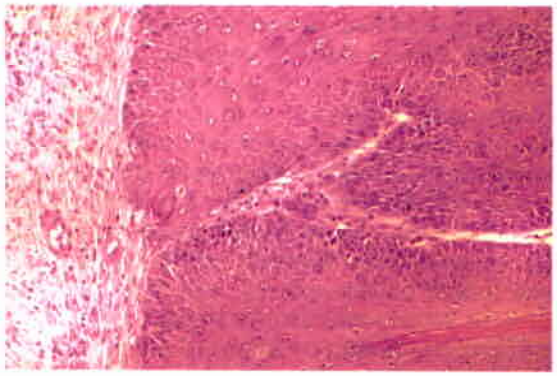

Figure 11

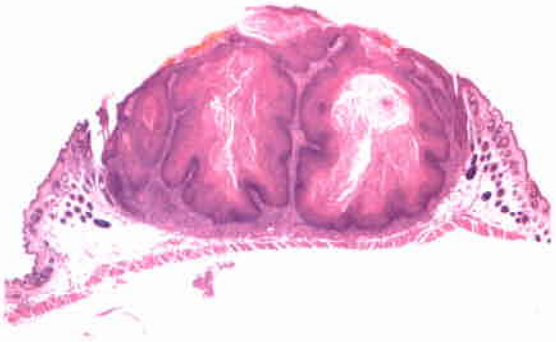

Figure 12

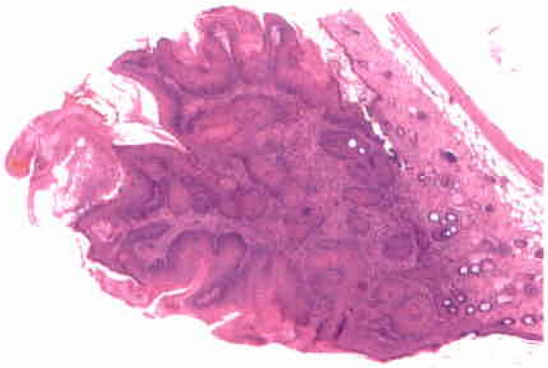

Figure 13

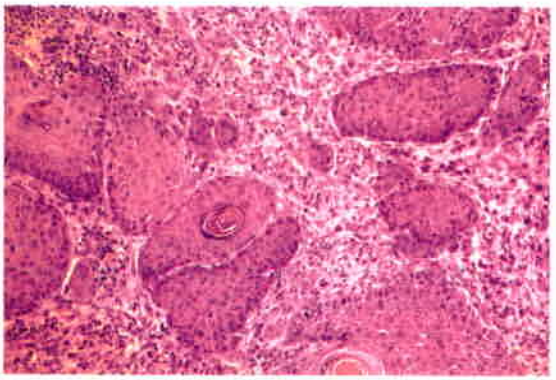

Figure 14

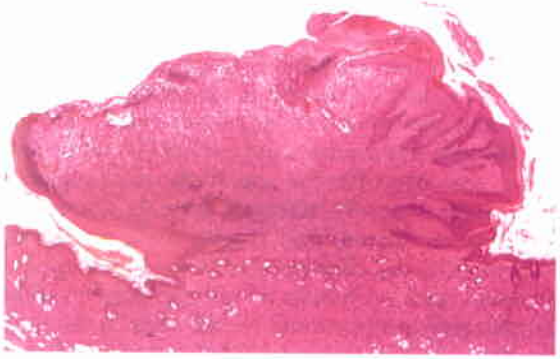

Figure 15

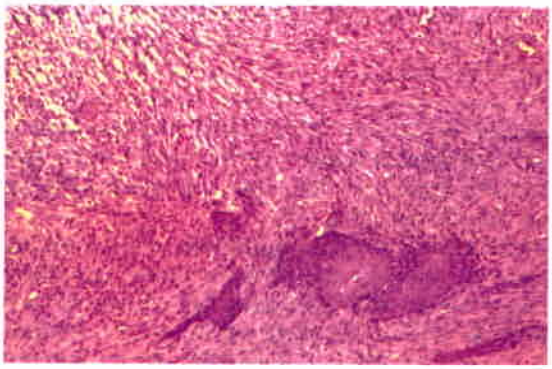

Figure 16

Several Tg.AC control females had benign teratomas of the ovary, consisting primarily of neural and/or cystic epithelial components. Malignant lymphoma was found in 2 control female Tg.AC mice, 1 presenting as a thymic mass and 1 with primarily spleen involvement. Single incidences of several tumor types were observed in control female Tg.AC mice. These were endometrial adenoma, uterine histiocytic sarcoma, small intestinal carcinoma, and subcutis mast cell tumor.

The incidence of tumors seen in control $p53^{+/-}$ mice was less than that seen in Tg.AC mice, and the spectrum of tumor types was also less varied. The majority of tumors seen in controls, and the only 2 neoplastic effects of chemical treatment observed in $p53^{+/-}$ mice (see below), were subcuticular sarcomas and systemic malignant lymphomas. Sarcomas of the subcutis were comprised of poorly differentiated spindle to epithelioid cells cytologically similar to those of the treatment-related sarcomas described below. Four of the 6 subcuticular sarcomas found in male and female control $p53^{+/-}$ mice occurred in a single study (diethylstilbestrol) in which vehicle was administered by subcutaneous injection. Malignant lymphoma was found in 2 control $p53^{+/-}$ mice of each sex. A thymic mass or enlargement with 1 or more enlarged lymph nodes was the most common gross manifestation of lymphoma, and microscopically there was neoplastic effacement of these tissues as well as widespread visceral infiltration. Cytologically, the neoplastic cells were of the lymphoblastic type with pleomorphic vesicular nuclei and scant-to-moderate amounts of eosinophilic cytoplasm. Two control $p53^{+/-}$ mice had gross tumors of the skull that microscopically were osteosarcomas, 1 of the maxilla and 1 of the mandible. All other tumors found in control $p53^{+/-}$ mice occurred at single incidences: granulocytic leukemia and urinary bladder fibrosarcoma in males and lung AB adenoma and meningeal sarcoma in females.

Proliferative Treatment Effects After 6 Mo in Tg.AC Mice

Skin Tumors. Multiple proliferative epidermal lesions were observed grossly at the site of chemical application (SOA) in 7 of 12 topical studies in Tg.AC mice (Fig. 9). Microscopically, these tumors most frequently corresponded to squamous cell papillomas, usually of the exophytic, pedunculated type (Fig. 10). Typical papilloma features were seen microscopically, including thickened, heavily keratinized, and well-differentiated stratified squamous epithelium with intact noninvasive basal layers (Fig. 11). Invariably there was a mild-to-moderate infiltrate of mixed inflammatory cells and mast cells within the fibrovascular stalk. Broad-based sessile papillomas were less common. Other benign skin tumors were diagnosed as keratoacanthomas when there was more prominent endophytic growth with cup-shaped invaginations into the dermis (Fig. 12).

In 3 topical Tg.AC studies, squamous cell carcinomas were a treatment effect at the SOA. In some, conversion from a benign tumor was evidenced by dysplastic nests of atypical cells within the stalk of otherwise well-differentiated papillomas (Figs. 13 and 14). More advanced progression to malignancy was characterized in some tumors by more extensive invasion of the underlying dermis by nests of squamous cells. In some skin tumors, malignant conversion was evidenced by an abrupt transition from the well-differentiated papilloma epithelium to spindle cells, which filled the stalk, interpreted to be an anaplastic spindle cell carcinoma (Figs. 15 and 16).

Forestomach Tumors. Increased incidence and multiplicity of forestomach squamous cell papillomas were clearly related to topical treatment of Tg.AC mice in 1 study (melphalan). Forestomach papillomas were pedunculated, exophytic growths arising from the squamous epithelium, morphologically identical to those of the epidermis described above.

Lung Tumors. An increase in incidence and multiplicity of lung AB tumors was associated with topical treatment of Tg.AC mice with 1 of the chemicals (melphalan). The spectrum and continuum of proliferative lung lesions commonly seen in mice (hyperplasia, adenoma, and carcinoma) were found in this study, and AB tumors had papillary growth patterns (Fig. 17). Only a single lung tumor was noted grossly, which corresponded to the only AB carcinoma observed microscopically in this study.

Malignant Lymphoma. The incidence of malignant lymphoma increased in treated male Tg.AC mice of 1 study (cyclosporin). Grossly, affected animals had enlarged lymph nodes, spleens, and thymuses, which corresponded microscopically to typical morphology of architectural effacement by sheets of neoplastic round cells. Cytologically, the neoplastic cells were of the small, well-differentiated lymphocytic type. The site of origin could not be definitively determined due to disseminated involvement. In the spleen, the white pulp was expanded and neoplastic cells spilled over into the red pulp (Fig. 18). In the liver, there was a prominent hypercellularity due to diffuse sinusoidal infiltration by neoplastic cells as well as focal perivascular and periportal cellular accumulations (Fig. 19). Neoplastic infiltrates also were typically seen dissecting along mediastinal planes from the thymus and mediastinal nodes into the lungs and infiltrating the interstitium of the kidney.

Myelodysplasia. An unusual systemic myeloproliferative and infiltrative effect was associated with treatment in 1 study (rotenone) in Tg.AC mice. This effect was characterized by excessive numbers of a mixture of immature hematopoietic cells and mature granulocytes and mononuclear cells in multiple organs, most commonly in the liver, spleen, lymph nodes, and bone marrow, and to a lesser extent in the lungs, kidneys, stomach, and other organs. Depending on the site and severity, the lesions of this disorder had variable features of hematopoietic, inflammatory, and/or neoplastic processes. Because the lesions were considered to represent both a morphological and biologic continuum, the collective term "myelodysplasia" was used for the spectrum of changes observed. In the more severely affected animals there was grossly evident liver, spleen, and lymph node enlargement. Microscopically, the changes in the liver were typically most consistent and the extent of involvement in other organs was generally proportional to that seen in the liver. Therefore, the severity of liver changes was used as the basis for grading of myelodysplasia in affected animals. Min-

imal to mild severity was characterized by randomly scattered foci of perivascular, periportal, and sinusoidal mixed cell infiltration. The infiltrates were composed of mature granulocytes, especially eosinophils, and mononuclear cells, including plasma cells. Subendothelial cell infiltrates often caused a prominent bulging into the lumen of central veins (Fig. 20). Periportal infiltrates became more prominent with increased severity and cells extended beyond the limiting plate. Hyaline degeneration and proliferation of bile ducts was a distinguishing change seen in tissues with portal involvement (Fig. 21). Severity of myelodysplasia was graded moderate to marked when infiltration became bridging and coalescing and when it replaced a significant amount of hepatic parenchyma. Perivascular fibrosis was generally more prominent in the more severely affected animals (Fig. 22), and the infiltrate often had a greater component of immature granulocytes (Fig. 23) as well as plasma cells, mast cells, and occasional megakaryocytes. Erythropoietic foci could also be found in the sinusoids.

The spleen of severely affected mice generally had lymphoid depletion of the white pulp and replacement by mixed cell infiltrates similar to those found in the liver. Both erythropoiesis and granulopoiesis were increased in the red pulp. The bone marrow was usually hypercellular with an increased myeloid:erythroid ratio, mostly due to an abundance of mature myeloid cells, and occasional megakaryocytosis and plasmacytosis. Enlarged lymph nodes were due to marked medullary plasmacytosis and variable degrees of infiltration by myeloid cells. Perivascular infiltrates in the lungs, kidneys, and other organs were often more mononuclear in composition than those in the liver and spleen.

Proliferative Treatment Effects After 6 Mo in $p53^{+/-}$ Mice

A neoplastic effect was observed in only 1 $p53^{+/-}$ mouse study (melphalan). However, in this study, 2 tumor types were associated with treatment.

Subcutis Sarcomas. Masses involving the subcutis, abdominal wall, and viscera of the caudal abdominal cavity in the region of the intraperitoneal injection sites were grossly observed in several $p53^{+/-}$ mice. Microscopically, the masses were generally composed of either interlacing bundles of poorly differentiated spindle cells or more pleomorphic and anaplastic cell types, including giant cells with single or multiple nuclei (Fig. 24). Although a definite site of origin could often not be determined due to the size and extensive local involvement of the neoplasm, these tumors were presumed to have originated in the subcutis and to have invaded through the abdominal wall into the peritoneal cavity. Adhesions between bowel segments due to inflammatory or neoplastic cells were common. Although a particular tumor may have had features more suggestive of fibrosarcoma, rhabdomyosarcoma, or malignant fibrous histiocytoma, all of these tumors were collectively diagnosed as sarcoma, NOS (not otherwise specified) pending further characterization by electron microscopy or immunohistochemistry.

Malignant Lymphoma. In the same study as described above, there was an increased incidence of malignant lymphoma in male $p53^{+/-}$ mice. The most common treatment-related gross observations in these animals were enlarged lymph nodes and thymus or presence of a thymic mass. The spleen was less consistently enlarged. Microscopically, malignant lymphoma in $p53^{+/-}$ mice presented a similar cytomorphology and multicentric organ involvement pattern as seen in control $p53^{+/-}$ mice of this and other (7) reports.

Discussion

Neoplastic target organs observed in these chemical studies were the skin SOA, forestomach, lung, and lymphohematopoietic system in Tg.AC transgenic mice (7 studies) and the lymphoid system and the site of injection in soft tissues in $p53^{+/-}$ mice (1 study). It was not unexpected that the skin SOA was the most frequent target in Tg.AC mice, given the fact that the epidermal cells exposed to the chemical can be considered genetically initiated by the activated *ras* transgene and that the development of skin papillomas is the primary reporter phenotype of chemical exposure in this strain (21). Benign tumors with morphological characteristics of keratoacanthoma were also present. Progression of benign skin tumors to carcinomas was clearly seen in this set of studies, consistent with the reported sensitivity of both the Tg.AC line (10) and the FVB/N background strain (11) to malignant conversion of skin papillomas. Malignant conversion of papillomas was often detected only by careful microscopic examination and by the presence of subtle nests of dysplastic cells beneath the otherwise intact and well-differentiated epithelium of the papilloma. Deeper dermal invasion by disorganized nests and cords of squamous cells characterized the more advanced carcinomas. A spindle cell tumor devoid of keratinocytic differentiation was found within the stalk of 1 papilloma and was interpreted to be an anaplastic spindle cell carcinoma. Although spindle cell tumors in the skin of Tg.AC mice have been diagnosed by light microscopy as sarcomas (3), electron microscopic examination and keratin immunostaining of a set of these tumors from Tg.AC mice have demonstrated epithelial characteristics (1). A low incidence of spontaneous skin tumors has been reported in Tg.AC mice, presumably from trauma and grooming activity (20), and was also seen in the current studies.

Although the skin tumors are regarded to be the primary tumor end point in Tg.AC mice, internal sites were also found to be neoplastic targets in this set of studies. These new target organs were the forestomach, lung, and lymphohemopoietic system. Forestomach papillomas were a treatment effect in 2 studies, 1 a gavage study in which there was direct chemical exposure to the forestomach epithelium and 1 a topical study in which exposure was likely secondary to grooming activity. Similar to skin papillomas, forestomach papillomas also occur naturally in Tg.AC mice with relatively high frequency, perhaps due to nonspecific irritation by ingested material. In general, the incidence of forestomach papilloma in controls was 1–2 animals from groups of 15. However, in 1 study, 6 of 14 male and 9 of 15 female control Tg.AC mice had this tumor. At present it is unclear whether this reflects a marked variability to be expected

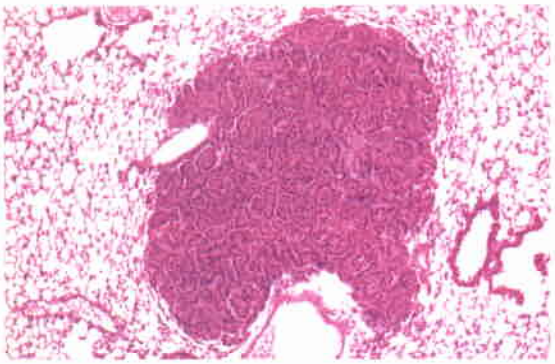

Figure 17

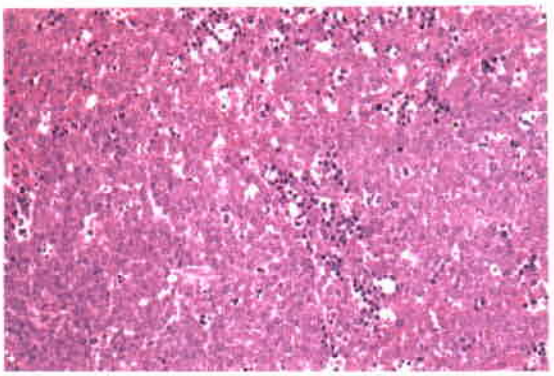

Figure 18

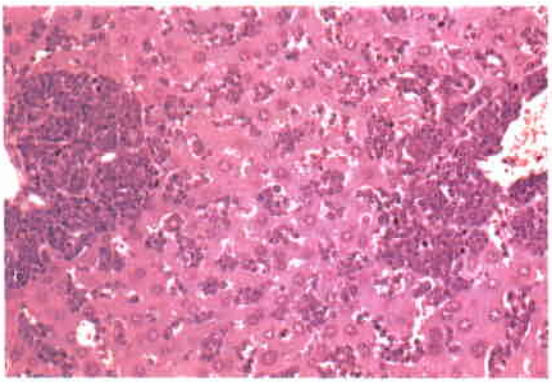

Figure 19

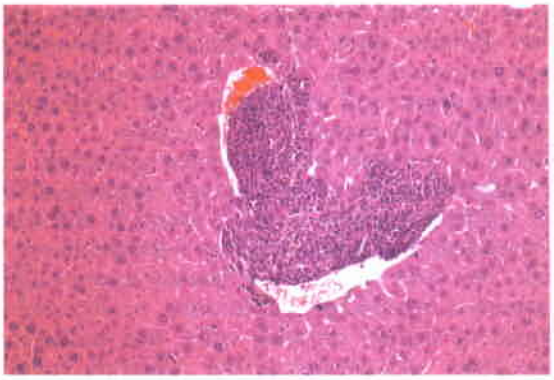

Figure 20

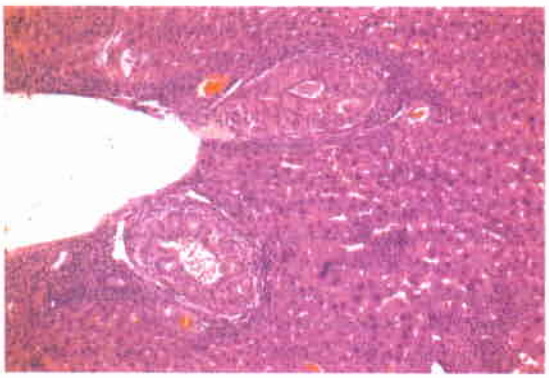

Figure 21

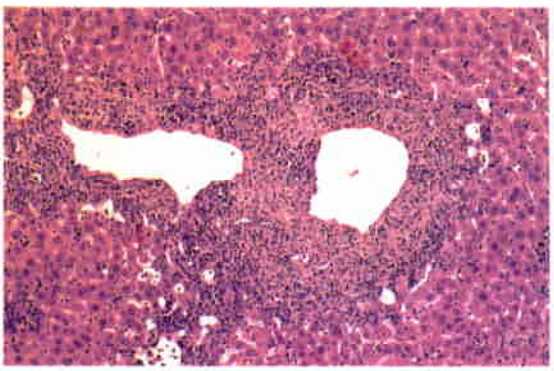

Figure 22

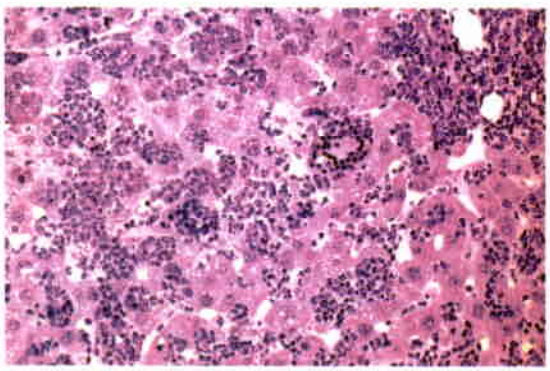

Figure 23

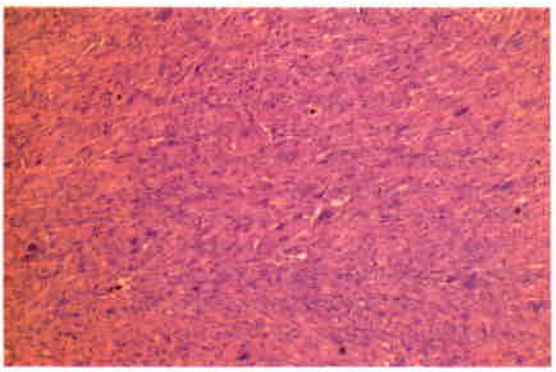

Figure 24

in the spontaneous occurrence of this tumor or whether it was an unusual and spurious occurrence in this particular study. While skin tumors are presumed to arise from the follicular epithelium, forestomach papillomagenesis indicates that nonfollicular squamous epithelium can also be a site of origin.

Proliferative lesions of the lung arose spontaneously and as a chemical effect in Tg.AC mice. Typical AB adenomas and carcinomas were seen in addition to preneoplastic alveolar cell hyperplasia. AB tumors are the most common neoplasm in aging FVB/N strain mice (18), the founder strain for the Tg.AC line. Reduced latency of these tumors may be both a transgene and a chemical effect in Tg.AC mice, resulting in both the naturally occurring and treatment-related tumors in these relatively young animals.

As in many mouse strains, malignant lymphoma is also a relatively common spontaneous and chemically induced tumor in Tg.AC and *p53*$^{+/-}$ mice. Accelerated lymphomagenesis has been reported as an effect in *p53*$^{+/-}$ mice following chemical exposure to phenolphthalein (7) and radiation (15), and the morphological expression of this effect is similar to that found in the single positive study in this report. To our knowledge, this is the first report of a lymphomagenic response in Tg.AC mice. The lymphoma incidence in *p53*$^{+/-}$ control mice of the current studies was greater than that in Tg.AC control mice, as was the proportion with primarily thymic involvement. The occurrence of lymphoma in the controls of our current studies and that of osteosarcoma is in agreement with the findings of Donehower et al (6), who found osteosarcomas and lymphomas, mostly of the thymic type, to be the most common neoplasms in aging *p53*-deficient heterozygotes.

As might be expected from the known ability of *ras* activation to transform hematopoietic cells (16) and the globin promoter of the transgene construct, proliferative hematopoietic disorders other than lymphoma were observed in Tg.AC mice. One of these was erythroleukemia, a naturally occurring hematopoietic neoplasm in this transgenic line that is rare in other mouse strains or species (9). Grossly, erythroleukemia and lymphoma may both cause enlargements of the liver, spleen, and lymph nodes that microscopically correspond to infiltration by mononuclear cells. In contrast to lymphoma, however, the liver is the most consistently and severely affected organ in erythroleukemia of Tg.AC mice. Definitive diagnosis can be made only by carefully examining for cytological features of erythrodifferentiation, the most important of which is the presence of nucleated red cells admixed with more undifferentiated cells (erythroblasts). The ratio of erythroblasts to more mature nucleated red cells may vary from case to case. Erythroblasts have slightly more basophilic cytoplasm than lymphoid cells. Blood vessels were hypercellular in histological sections; although hematologic analysis was not done in the studies described in this report, we have found involvement of the peripheral blood, with markedly increased numbers of circulating metarubricytes and erythroblasts, in all animals examined hematologically (Mahler et al, unpublished observations). The pathogenesis of erythroleukemia in Tg.AC mice is still under investigation but undoubtedly is associated with the transgene, since this neoplasm is so rare and has never been seen in the FVB/N background strain (18). Targeted overexpression of *ras* in erythroid precursors caused by the ζ-globin promoter may be involved (5, 16). There should be suspicion of erythroleukemia in all cases of hepatomegaly seen in Tg.AC mice, and blood smears can be useful as a simple diagnostic aid in distinguishing this neoplasm from lymphoma.

Another hematopoietic disorder found in Tg.AC mice that must be considered along with lymphoma and erythroleukemia in the differential diagnosis of systemic infiltrating disease is a spectrum of lesions that we have termed myelodysplasia. This is perhaps the most unusual disorder as well as the most problematic one encountered in these studies from a diagnostic and interpretive standpoint. This was seen only as a treatment effect in 1 study. The histomorphology of this disorder is unique, and its biology is unknown; therefore, the term myelodysplasia was selected to reflect both its ambiguous morphological appearance and its biologic behavior. In addition, the disease in Tg.AC mice has many of the morphological manifestations of the myeloproliferative diseases in humans and cats (13) characterized by aberrant proliferations of 1 or more hematopoietic lineages and considered to be "preleukemic." The lesions of myelodysplasia in Tg.AC mice may have features of an inflammatory, hematopoietic, or neoplastic process. The perivascular infiltration pattern, particularly in milder cases, and the well differentiated characteristics of the infiltrating cells suggest an inflammatory process. In more severe instances, there is a more leukemic-like infiltration, particularly in the liver, and the appearance of granulocytopoietic foci, although most of the infiltrating cells remain well differentiated. Eosinophils are usually a prominent component of the granulocyte infiltrate, and the fibrosis evident in the liver may be the result of elaboration of cytokines, such as transforming growth factor beta, by these cells (14). The peripheral blood profile of this disorder in Tg.AC mice has not yet been characterized.

←

FIGS. 17–24.—17) Typical AB adenoma seen as spontaneous and treatment-related tumors in Tg.AC mice. This tumor exhibits a papillary growth pattern. 18) Lymphoma in the spleen of a Tg.AC mouse. Neoplastic cells infiltrate between dark-staining erythropoietic foci of the red pulp. 19) Lymphoma in the liver of a Tg.AC mouse. Neoplastic cells diffusely fill the sinusoids and portal tracts. 20) Partial veno-occlusion due to myelodysplastic infiltration. 21) Hyperplastic bile ducts with hyaline degeneration and more extensive lobular infiltration in a Tg.AC mouse with myelodysplasia. 22) Perivascular cellular infiltration and fibrosis of severe myelodysplasia in a Tg.AC mouse. 23) Severe sinusoidal infiltration of myelodysplasia including numerous foci of eosinophilic granulocytopoiesis. 24) Poorly differentiated spindle cell sarcoma of the subcutis in a *p53*$^{+/-}$ mouse with spindle and multinucleated giant cells.

The etiology and the toxicologic significance of myelodysplasia in the Tg.AC line are unknown. In many mouse strains, the response to inflammatory stimuli, especially in the skin, may be exuberant granulocyte proliferation, and criteria for distinguishing severe myeloid hyperplasia from granulocytic leukemia have been proposed (17). Myelodysplasia has been observed in previous Tg.AC skin paint studies in which an association between its occurrence and the burden of skin papillomas was made (Mahler et al, unpublished observations), suggesting that the myeloproliferation was due to cytokines, which have been shown to be released from mouse epidermal tumor cells (2). However, in the current study, in which myelodysplasia was an effect, there was no skin papilloma response. Until more is known about the biology of this disorder, its toxicologic implications remain unclear.

Besides malignant lymphoma, induction of soft tissue sarcomas was the only other treatment effect seen in *p53*$^{+/-}$ mice. In the single study in which they occurred, the sarcomas arose at sites of intraperitoneal injection. Sarcoma cells generally were extemely pleomorphic and undifferentiated and therefore were not subclassified pending further characterizations. Site-of-injection sarcomas arose in vehicle (propylene glycol)–injected controls as well as in treated animals, suggesting that they were secondary to nonspecific mechanisms and that they were not a direct chemical effect. This is further supported by observations that sarcomas may arise in *p53*$^{+/-}$ mice at subcutaneous sites of foreign body implantation (Mahler et al, unpublished observations). However, induction of soft tissue sarcomas is a reported oncogenic effect of radiation in heterozygous *p53*-deficient mice (15), and we have seen subcutaneous sarcomas induced in this strain by a gavage study of benzene (Mahler et al, unpublished observations). Therefore, soft tissue sarcomas and lymphomas may be expected to be common treatment effects in studies with this line of mice. A low incidence of subcutis sarcomas was observed in controls from other studies as well, in accordance with the findings of Donehower et al (6) that sarcomas are a relatively common spontaneous tumor in aging *p53*-deficient mice.

Although not seen in the current set of studies, other tissues have been shown to be the site of accelerated carcinogenic activity in short-term chemical exposures in *p53*-deficient mice (21), including the transitional epithelium of the urinary bladder and the epidermis. In another report (19), 35 weekly intraperitoneal injections of *p53*-deficient heterozyous mice with crocidolite asbestos fibers resulted in a 76% incidence of malignant mesothelioma with an average latency of 44 wk. In our studies, a mesothelioma was found on the serosal surface of the colon in a single treated *p53*$^{+/-}$ mouse injected intraperitoneally with the test chemical (melphalan), but a relationship to chemical treatment was not apparent from this low incidence.

As was anticipated, the incidence of spontaneous tumors in Tg.AC mice and *p53*$^{+/-}$ mice at termination of these 26-wk studies was much lower than that found in 2-yr bioassays. The low background tumor rate is in fact 1 of the strong arguments for the use of these genetically altered mice in short-term studies. The most common tumors were odontogenic neoplasms in the Tg.AC line at an incidence of approximately 15%. An increased incidence of these tumors was not seen in any of the studies reported here or in any others, to the best of our knowledge. Perhaps the tumors of most concern, as regards interpretion of chemical effects, are the skin and forestomach papillomas in Tg.AC mice and the lymphomas and sarcomas in *p53*$^{+/-}$ mice due to their relatively high frequency of occurrence in controls and because of their potential to obscure treatment effects. The incidence and multiplicity of papillomas in the Tg.AC studies interpreted as positive in this current data set were sufficiently increased over the occurrence in controls to allow us to make definitive calls. Likewise, our data demonstrate that lymphomas and sarcomas are unlikely to occur in greater than single incidences in standard groups of 15–20 control heterozygous *p53*-deficient mice, thereby facilitating interpretation of chemical carcinogenic activity.

In summary, these studies demonstrate a variety of neoplastic target organ effects in Tg.AC and *p53*$^{+/-}$ mice. Some of these target sites were expected from previous findings, such as skin tumors in the Tg.AC line and lymphomas in the *p53*-deficient line. However, unexpected targets were observed in this set of studies, most notably the forestomachs, hematopoietic systems, and lungs of Tg.AC mice. Some of these novel targets were only discovered by microscopic examination, indicating the need for at least some degree of histologic evaluation of treated animals. The current studies also demonstrate the occurrence of some lesions, both spontaneous and treatment-related, with unusual and unique morphologies. The use of these new animal models in hazard identification will therefore present both an exciting and challenging new role for the toxicologic pathologist.

ACKNOWLEDGMENTS

The authors gratefully acknowledge the expertise of the following pathologists for their evaluation and review of the pathology data: Drs. R. Hailey, A. Radovsky, and J. Leininger (NIEHS); Dr. M. Elwell (Experimental Pathology Laboratories, Inc.); and Drs. L. Lanning, M. Jokinen, and J. Nold (Pathology Associates International). Gratitude is also expressed to Drs. J. Bucher and R. Maronpot (NIEHS) for their critical review of the manuscript. Photographic materials for Fig. 1 and the cover illustration were kindly provided by C. Trempus, J. French, and S. McCaw of NIEHS.

REFERENCES

1. Asano S, Trempus CS, Spalding JW, Tennant RW, and Battalora MS (1998). Morphological characterization of spindle cell tumors induced in transgenic Tg.AC mouse skin. *Toxicol. Pathol.* 26: 512–519 (this issue).
2. Bauluz C, Larcher F, Ballestin C, Grande T, and Jorcano J (1994). Augmented expression of cytokines in mouse epidermal tumor cells and its possible involvement in the induction of hematopoietic alterations. *Mol. Carcinog.* 11: 155–163.
3. Cardiff RD, Leder A, Kuo A, Pattengale PK, and Leder P (1993). Multiple tumor types appear in a transgenic mouse with the ras oncogene. *Am. J. Pathol.* 142: 1199–1207.
4. Chhabra RS, Huff JE, Schwetz BS, and Selkirk J (1990). An over-

view of prechronic and chronic toxicity/carcinogenicity experimental study designs and criteria used by the National Toxicology Program. *Environ. Health Perspect.* 86: 313–321.

5. Cline MJ (1994). The molecular basis of leukemia. *N. Engl. J. Med.* 330: 328–336.
6. Donehower LA, Harvey M, Vogel H, McArthur MJ, Montgomery CA, Park SH, Thompson T, Ford RJ, and Bradley A (1995). Effects of genetic background on tumorigenesis in p53-deficient mice. *Mol. Carcinog.* 14: 16–22.
7. Dunnick JK, Hardisty JF, Herbert RA, Seely JC, Furedi-Machacek EM, Foley JF, Lacks GD, Stasiewicz S, and French JE (1997). Phenolphthalein induces thymic lymphomas accompanied by loss of the p53 wild type allele in heterozygous p53-deficient mice. *Toxicol. Pathol.* 25: 533–540.
8. Eastin WC, Haseman JK, Mahler JF, and Bucher JR (1998). The National Toxicology Program evaluation of genetically altered mice as predictive models for identifying carcinogens. *Toxicol. Pathol.* 26: 461–473 (this issue).
9. Frith CH, Ward JM, and Chandra M (1993). The morphology, immunohistochemistry, and incidence of hematopoietic neoplasms in mice and rats. *Toxicol. Pathol.* 21: 206–218.
10. Hansen LA, Trempus CS, Mahler JF, and Tennant RW (1996). Association of tumor development with increased cellular proliferation and transgene overexpression, but not c-Ha-*ras* mutations, in v-Ha-*ras* transgenic Tg.AC mice. *Carcinogenesis* 17: 1825–1833.
11. Hennings H, Glick AB, Lowry DT, Krsmanovic LS, Sly LM, and Yuspa SH (1993). FVB/N mice: An inbred strain sensitive to the chemical induction of squamous cell carcinomas in the skin. *Carcinogenesis* 14: 2353–2358.
12. Huff J, Cirvello J, Haseman J, and Bucher J (1991). Chemicals asociated with site-specific neoplasia in 1394 long-term carcinogenesis experiments in laboratory rodents. *Environ. Health Perspect.* 93: 247–270.
13. Jain NC (1993). The leukemias: General aspects. In: *Essentials of Veterinary Hematology,* NC Jain (ed). Lea and Febiger, Philadelphia, pp. 326–333.
14. Kadin M, Butmarc J, Elovic A, and Wong D (1993). Eosinophils are the major source of transforming growth factor beta 1 in nodular sclerosing Hodgkin's disease. *Am. J. Pathol.* 142: 11–16.
15. Kemp CJ, Wheldon T, and Balmain A (1994). p53-Deficient mice are extremely susceptible to radiation-induced tumorigenesis. *Nat. Genet.* 8: 66–68.
16. Liu ET (1990). The role of *ras* gene mutations in myeloproliferative disorders. *Clin. Lab. Med.* 10: 797–807.
17. Long RE, Knutsen G, and Robinson M (1986). Myeloid hyperplasia in the SENCAR mouse: Differentiation from granulocytic leukemia. *Environ. Health Perspect.* 68: 117–123.
18. Mahler JF, Stokes W, Mann PC, Takaoka M, and Maronpot RR (1996). Spontaneous lesions in aging FVB/N mice. *Toxicol. Pathol.* 24: 710–716.
19. Marsella JM, Liu BL, Vaslet CA, and Kane AB (1997). Susceptibility of p53-deficient mice to induction of mesothelioma by crocidolite asbestos fibers. *Environ. Health Perspect.* 105(suppl. 5): 1069–1072.
20. Spalding JW, Momma J, Elwell MR, and Tennant RW (1993). Chemically induced skin carcinogenesis in a transgenic mouse line (TG.AC) carrying a v-Ha-ras gene. *Carcinogenesis* 14: 1335–1341.
21. Tennant RW, French JE, and Spalding JW (1995). Identifying chemical carcinogens and assessing potential risk in short-term bioassays using transgenic mouse models. *Environ. Health Perspect.* 103: 942–950.
22. Wright JT, Hansen L, Mahler J, Szczesniak C, and Spalding JW (1995). Odontogenic tumours in the v-Ha-*ras* (TG.AC) transgenic mouse. *Arch. Oral Biol.* 40: 631–638.